JOURNAL OF CATALYSIS 149, 11–22 (1994)

^{15}N Labeling Studies of the Reduction of Nitric Oxide by Ammonia over Amorphous and Crystalline Chromia in the Presence and Absence of Oxygen

Bronwyn L. Duffy,* H. Edward Curry-Hyde,* Noel W. Cant,† and Peter F. Nelson‡

*School of Chemical Engineering and Industrial Chemistry, University of New South Wales, Kensington, New South Wales 2033, Australia; †School of Chemistry, Macquarie University, New South Wales 2109, Australia; and ‡CSIRO Division of Coal and Energy Technology, P.O. Box 136, North Ryde, New South Wales 2113, Australia

Received September 29, 1993; revised March 18, 1994

Isotopic labeling studies of the reaction between ^{15}NO and $^{14}NH_3$ have been performed, under selective catalytic reduction (SCR) conditions, for amorphous and crystalline chromia catalysts over a wide range of temperatures (140–350°C) and oxygen concentrations (0–1.8% O_2). At low temperatures, and with 1.8% O_2, nitrogen is formed largely by the selective reduction of NO and NH_3 over both catalysts. However, crystalline chromia has a much higher activity for ammonia oxidation. Thus, at ≈200°C, the major form of nitrogen produced by amorphous chromia is $^{14}N^{15}N$, whereas, for crystalline α-Cr_2O_3, nitrogen is mainly $^{14}N_2$ and is therefore produced largely from ammonia oxidation. The dominant form of nitrous oxide produced in the presence of O_2 over both morphologies of chromia is always $^{14}N^{15}NO$. Thus, formation of N_2O, an undesirable product, involves the reaction of one molecule of NO and one molecule of NH_3. It has been shown that Fourier transform infrared (FTIR) spectroscopy can be used to distinguish between $^{14}N^{15}NO$ and $^{15}N^{14}NO$. In the presence of excess O_2, NO decomposition is unimportant for both catalysts. In the absence of O_2, very similar product distributions are observed for the two morphologies of chromia. The dominant form of nitrogen is $^{14}N^{15}N$, but the nitrous oxide is largely $^{15}N_2O$, and therefore formed by NO decomposition. Evidence is presented for some conversion of N_2O to N_2 in the absence of oxygen by a reaction conforming to $3N_2O + 2NH_3 \rightarrow 4N_2 + 3H_2O$. This reaction increases in importance with temperature. Concentrations of O_2 comparable to the NO and NH_3 concentrations (i.e., ≈1000 ppm) are sufficient to prevent the NO decomposition reactions, implying that O_2 effectively competes with NO for the available adsorption sites. Product distributions obtained in the presence of small amounts of O_2 are very similar to those achieved with excess O_2.

INTRODUCTION

Selective catalytic reduction (SCR) with ammonia is the most effective method for postcombustion control of emissions of nitrogen oxides from stationary sources (1). The currently favored catalysts are based on V_2O_5 and are usually operated at 350 to 400°C. Development of an active low-temperature SCR catalyst is attractive because it may allow greater flexibility in the placement of the SCR reactor in the flue gas stream and thus has the potential to reduce overall cost and improve efficiency.

Recently, amorphous chromia has been shown to be a highly active and selective catalyst for the reduction of nitric oxide with ammonia in the presence of excess oxygen (2). Over 90% conversion of nitric oxide was achieved at 140°C, whereas a typical industrial V_2O_5/TiO_2 catalyst requires 240°C to achieve the same conversion under the same conditions (2). The performance of chromia is, however, highly dependent on the morphology (3). Amorphous chromia produces nitrogen with very high selectivity below 180°C. Operation at higher temperature yields increasing amounts of less desirable nitrous oxide but the NH_3 : NO conversion ratio remains near 1 : 1, as expected for the stoichiometric reactions

$$4NH_3 + 4NO + O_2 \rightarrow 4N_2 + 6H_2O \quad [1]$$

$$4NH_3 + 4NO + 3O_2 \rightarrow 4N_2O + 6H_2O. \quad [2]$$

By contrast, crystalline chromia (α-Cr_2O_3) gives rise to substantial nitrous oxide at all temperatures, as was noted in early studies (4–6), and the NH_3 consumption greatly exceeds that of NO, which indicates the ammonia oxidation is a dominant side reaction. The differences in catalytic behavior of the two unsupported chromia catalysts have been rationalized in terms of morphology and surface structure (7).

The principal aim of the present work was to use ^{15}N labeling to answer two specific questions concerning the origin of the nitrogen atoms in the nitrous oxide and molecular nitrogen products formed over chromia catalysts in the presence of oxygen. First, are the increasing amounts of nitrous oxide formed at higher temperatures over amorphous chromia derived by a combination reac-

0021-9517/94 $6.00

tion involving NO and NH_3, or by an inherently different reaction, and hence amenable to separate control? Second, does the direct ammonia oxidation which occurs over crystalline α-Cr_2O_3 produce nitrogen and/or nitrous oxide?

Isotopic labeling techniques have substantially increased understanding of the SCR reaction over various oxide catalysts (8–14). However, there are considerable variations in the overall isotopic distributions which may reflect the wide choice of operating conditions and catalyst forms used by different authors. Only the experiments of Janssen *et al.* (8) and of Vogt *et al.* (9, 10) for vanadia-based catalysts have approximated industrial conditions. Previous studies using α-Cr_2O_3 and Cr_2O_3/Al_2O_3 systems by Niiyama *et al.* (11–13) were carried out in a recirculating or temperature-programmed system in the absence of oxygen and with nitric oxide and ammonia pressures in the multi-Torr range. The present work has employed a continuous flow system with low reactant pressures ($\approx$1000 ppm) and temperatures from 140 to 350°C to simulate possible industrial practice. In addition, the role of oxygen in the SCR reaction has not been fully clarified, and therefore, isotopic product distributions were determined for a wide range (0–1.8%) of oxygen concentrations. While the isotopic results show some similarities to earlier work, the use of a wide range of temperatures and oxygen concentrations has established observations and trends not previously evident.

EXPERIMENTAL METHODS

Catalytic testing was carried out in a continuous flow system in a manner described in detail elsewhere (15). In essence, NO and NH_3 (each with nominal concentration of 900 ppm) diluted with helium were passed over 25 to 600 mg of catalyst contained in a quartz tube of internal diameter 5 mm and heated to temperatures between 140 and 350°C. Three levels of oxygen concentration were used: absence (<5 ppm), small amounts ($\approx$1000 ppm), and excess ($\approx$18,000 ppm = 1.8%) oxygen. The exit gas was monitored continuously by a mass spectrometer with periodic sampling for analysis by gas chromatography and Fourier transform infrared (FTIR) spectroscopy. In experiments with ^{15}NO (Isotec Inc., 99.4% N), the catalyst was first run to a steady state with a $^{14}NH_3/^{14}NO$ mixture, and after the switch to ^{15}NO was made, the reaction was continued until the mass spectrometer signals were stable.

The quadrupole mass spectrometer was operated in multiple ion monitoring mode and component intensities calculated using a least-squares fitting procedure assuming fragmentation was unaffected by isotopic substitution. The least accurate analyses are for $^{14}N_2$ (due to a substantial background signal at *m/e* 28) and $^{15}N_2$, which is interfered with by ^{14}NO produced by oxidation of ammonia on the filament. With a low filament current (0.2 mA) ammonia oxidation was negligible with feeds free of oxygen, but reached the equivalent of $\approx$90 ppm for mixtures containing 900 ppm NH_3 and 18,000 ppm oxygen. Signals at *m/e* = 30 were adjusted for such contributions using a second order correction function established by regression of data obtained with calibration mixtures containing ^{15}NO.

FTIR was used to assess the amounts of ^{14}NO formed by the reaction of $^{15}NH_3$ versus $^{14}NH_3$, and of $^{14}N^{15}NO$ versus $^{15}N^{14}NO$. Direct $^{15}NO/^{14}NH_3$ isotopic exchange was discounted as $^{15}NH_3$ and ^{14}NO were never observed in the infrared spectra concurrently. Spectra were recorded at a resolution of 0.25 cm^{-1} on samples collected for off-line analysis by passing the product stream through a multiple reflection cell of total path length 3.2 m. Signal accumulation analyzing for NO and NH_3 was restricted to 16 scans, since the concentrations of these gases declined steadily with time due to a combination of oxidation of the former to NO_2 and adsorption or deposition on cell surfaces. Back extrapolation of infrared intensities to the time of collection showed that NO_2 concentrations were then less than 5% of the inlet NO concentration. Nitrous oxide concentrations were stable, which allowed the use of 256 scans to obtain better signal-to-noise ratios.

Conversions of ^{15}NO and NH_3 were determined from the mass spectral analyses of *m/e* = 31 and *m/e* = 17, respectively. The latter are less certain due to a contribution from fragment ions of H_2O and, in some cases, of $^{15}NH_3$. Conversions could also be obtained from the FTIR measurements using the sR (J = 10) line of $^{14}NH_3$ at 1176.6 cm^{-1} and the ^{15}NO line at 1851.2 cm^{-1}. In most cases, there was agreement to within $\pm$5% with similarly good agreement between the mass spectral and gas chromatographic analyses for total nitrogen and total nitrous oxides.

Chromia catalysts were prepared by addition of aqueous ammonia to a dilute solution of chromium (III) nitrate. The resultant precipitates were separated, dried overnight at 100°C in air, and decomposed by heating in a hydrogen flow. For amorphous chromia, the temperature was increased to a maximum temperature of 380°C (4°C/min, then isothermal for 3 h), whereas crystalline α-Cr_2O_3 was formed by heating to temperatures greater than 470°C. The preparations were crushed and sieved to 300–500 μm for the catalytic experiments. The surface areas, as determined by the BET method using a Quantachrome Model QS-17 surface area analyzer with nitrogen as the adsorbate, were 55 m^2/g (α-Cr_2O_3) and 280 m^2/g (amorphous chromia). The amorphous form was microporous with a large fraction of the total area in pores of diameter less than 2 nm. The average pore diameter of the α-Cr_2O_3

TABLE 1

Isotopic Product Distributions for the Reaction of ^{15}NO and $^{14}NH_3$ in the Presence of Excess (1.8 v/v%) Oxygen over Amorphous Chromia and α-Cr_2O_3

Catalyst	Temp. (°C)	Mass of catalyst (mg)	Flow rate (ml/min)	Conversion (%)		Selectivity to N_2O^a (%)	Product distribution (ppm)							$^{14}N^{15}NO/(^{14}N^{15}N + {}^{14}N^{15}NO)$ (%)
				^{15}NO	$^{14}NH_3$		$^{14}N_2$	$^{14}N^{15}N$	$^{15}N_2$[b]	$^{14}N_2O$	$^{14}N^{15}NO$	$^{15}N_2O$	^{14}NO	
Amorphous chromia	140	50	80	14	12	9	24	136	−21	2	14	0	<5	9
		125	40	77	67	5	43	630	−8	5	27	0	<5	4
	190	50	160	25	31	29	5	177	0	8	65	1	<5	27
		50	40	68	75	23	28	429	6	21	118	1	7	22
	195	50	160	35	42	30	26	218	−2	15	90	1	<5	29
		50	80	52	58	28	31	334	−7	29	117	1	5	26
α-Cr_2O_3	140	150	40	23	21	41	34	113	−1	2	102	0	<5	47
		600	33	69	67	44	18	310	13	6	249	1	<5	45
	185	50	120	25	37	63	53	36	−4	5	180	1	18	83
		100	80	41	76	66	107	68	7	34	361	2	20	84
		100	40	67	96	64	173	85	6	55	465	3	30	85

[a] Selectivity is defined as $(N_2O/(N_2 + N_2O + {}^{14}NO))$. Negatives are not included in the calculation.
[b] Determination difficult due to ammonia oxidation on the mass spectrometer filament.

was 30 nm. Crystal structures were confirmed by X-ray diffraction (XRD).

RESULTS AND DISCUSSION

Presence of Oxygen

Table 1 summarizes results for the reaction of equimolar amounts of ^{15}NO and $^{14}NH_3$ over both amorphous chromia and crystalline α-Cr_2O_3 in the presence of 1.8% (18,000 ppm) oxygen. Under these conditions, meaningful measurements became difficult above 200°C as the ammonia conversion was then near complete. In order to determine the effects of near stoichiometric O_2 concentrations on the product distributions, additional experiments were carried out with a much lower input oxygen concentration (≈0.1% = 1000 ppm). In these cases, inlet oxygen concentrations were chosen so that the conversion of oxygen was ≈50% across the catalyst bed. Low oxygen conditions also enabled the temperature range to be extended. The data are shown in Table 2.

Figures 1 and 2 summarize the isotopic distributions for nitrous oxide and nitrogen, respectively (as calculated from all the data of Tables 1 and 2). All values obtained by varying space velocity (and hence conversion) at each temperature are included and show that the isotopic product distributions were not greatly influenced by the degree of conversion. The results for nitrous oxide (Fig. 1) are very clear. Over both catalysts, under all conditions, more than 80% of the nitrous oxide is $^{14}N^{15}NO$, and thus derived by combination of ^{15}NO and $^{14}NH_3$. Ammonia oxidation to $^{14}N_2O$ amounts to 5–15% and the amount of $^{15}N_2O$, representing ^{15}NO decomposition, is very small.

Previous studies have relied on mass spectral fragmentation patterns to distinguish between $^{14}N^{15}NO$ and $^{15}N^{14}NO$. The distinction is made much more clearly by FTIR spectroscopy. Figure 3a shows the spectrum of the $^{14}N_2O$ product from a reaction of ^{14}NO and $^{14}NH_3$, while

TABLE 2

Isotopic Product Distributions for the Reaction of ^{15}NO and $^{14}NH_3$ in the Presence of Small Oxygen Concentrations (≈1000 ppm) over Amorphous Chromia and α-Cr_2O_3

Catalyst	Temp. (°C)	Mass of catalyst (mg)	Flow rate (ml/min)	Conversion (%)			Selectivity to N_2O^a (%)	Product distribution (ppm)								$^{14}N^{15}NO/(^{14}N^{15}N + {}^{14}N^{15}NO)$ (%)
				^{15}NO	$^{14}NH_3$	O_2		$^{14}N_2$	$^{14}N^{15}N$	$^{15}N_2$	$^{14}N_2O$	$^{14}N^{15}NO$	$^{15}N_2O$	$^{15}NH_3$[b]	^{14}NO[b]	
Amorphous chromia	190	50	40	47	42	36	40	20	178	−17	5	126	1	<5	<5	41
	220	50	60	39	46	44	60	25	97	2	21	194	5	<5	<5	25
	280	25[c]	80	46	84	56	62	52	88	10	55	282	2	<5	<5	59
α-Cr_2O_3	185	50	40	27	42	46	57	56	53	−9	2	141	1	<5	<5	73
	210	50	160	28	66	46	50	127	51	−3	3	171	1	<5	<5	77
	280	25[c]	80	40	97	49	51	156	38	23	34	277	2	<5	86	88

[a] Selectivity is defined as $(N_2O/(N_2 + N_2O + {}^{14}NO))$. Negatives are not included in the calculation.
[b] By FTIR spectroscopy.
[c] 25 mg of unsupported chromia diluted with 25 mg of TiO_2.

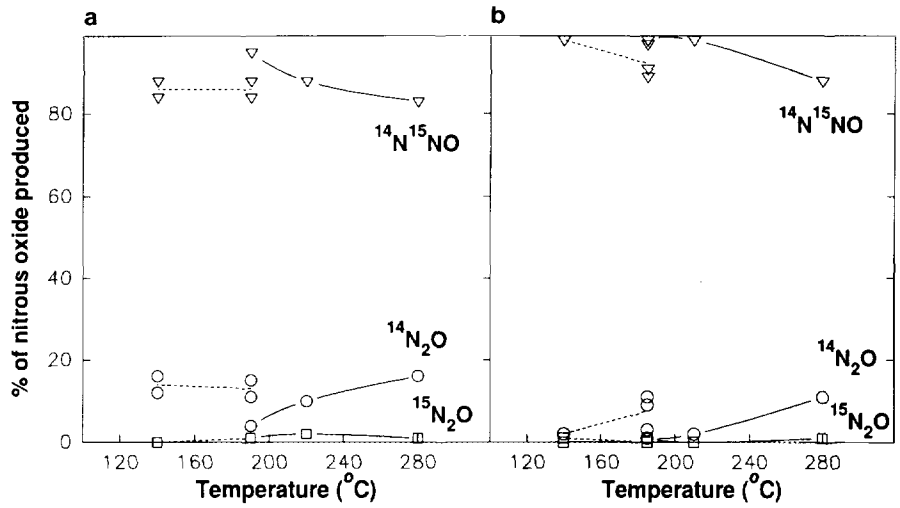

FIG. 1. Internal distribution of the nitrous oxides as a function of temperature ((○) $^{14}N_2O$; (▽) $^{14}N^{15}NO$; (□) $^{15}N_2O$) over (a) amorphous chromia and (b) α-Cr_2O_3. Points joined by dashed line, 1.8% O_2; points joined by full line, ≈1000 ppm O_2.

Fig. 3b is for the product of a corresponding ^{15}NO plus $^{14}NH_3$ reaction. The latter clearly shows a set of small peaks centered at 2223.8 cm^{-1}, which correspond to $^{14}N_2O$ (16), and which can be removed by subtraction of Fig. 3a with an appropriate scaling factor. The residual spectrum, Fig. 3c, shows a clean set of peaks centerd at 2177.7 cm^{-1} as expected for $^{14}N^{15}NO$ (17). There is no trace of features centered at 2201.6 cm^{-1}, where $^{14}N^{15}NO$ is expected to absorb (16). Similarly, bands due to the two other fundamental vibrations of $^{14}N^{15}NO$ were detectable at 1280.4 and 575.4 cm^{-1}, respectively, with no evidence of the corresponding bands of $^{15}N^{14}NO$ expected at 1269.9 and 585.3 cm^{-1}. Thus, all the nitrous oxide made from a combination of ^{15}NO and $^{14}NH_3$ retains the starting nitrogen–oxygen bond.

The isotopic results for nitrogen in Fig. 2 show that combination of ^{15}NO and $^{14}NH_3$ to form $^{14}N^{15}N$ is the major source of nitrogen at low temperature (at 140°C for α-Cr_2O_3 and below 200°C for amorphous Cr_2O_3). As the temperature increases $^{14}N_2$, which must arise from $^{14}NH_3$ oxidation, comprises an increasing proportion of the nitrogen formed over both catalysts. The trend is especially pronounced with α-Cr_2O_3, for which ammonia oxidation exceeds the combination reaction above 180°C and contributes 75% of the total nitrogen by 200°C.

Figures 1 and 2 show a fairly smooth transition between the two levels of oxygen concentration, which indicates that there is a minimum oxygen concentration threshold above which further increases have little effect on reaction pathways, and hence on product distribution. The only

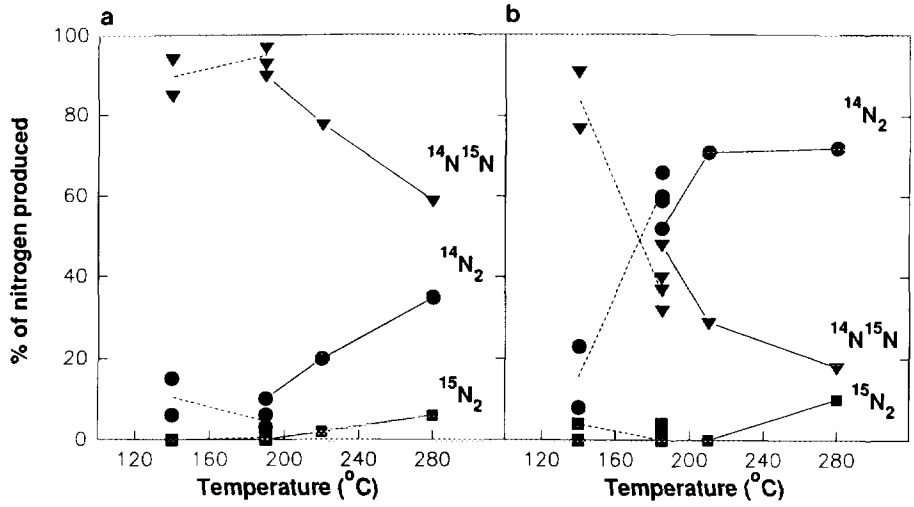

FIG. 2. Internal distribution of the nitrogens as a function of temperature ((●) $^{14}N_2$; (▼) $^{14}N^{15}N$; (■) $^{15}N_2$) over (a) amorphous chromia and (b) α-Cr_2O_3. Points joined by dashed line, 1.8% O_2; points joined by full line, ≈1000 ppm O_2.

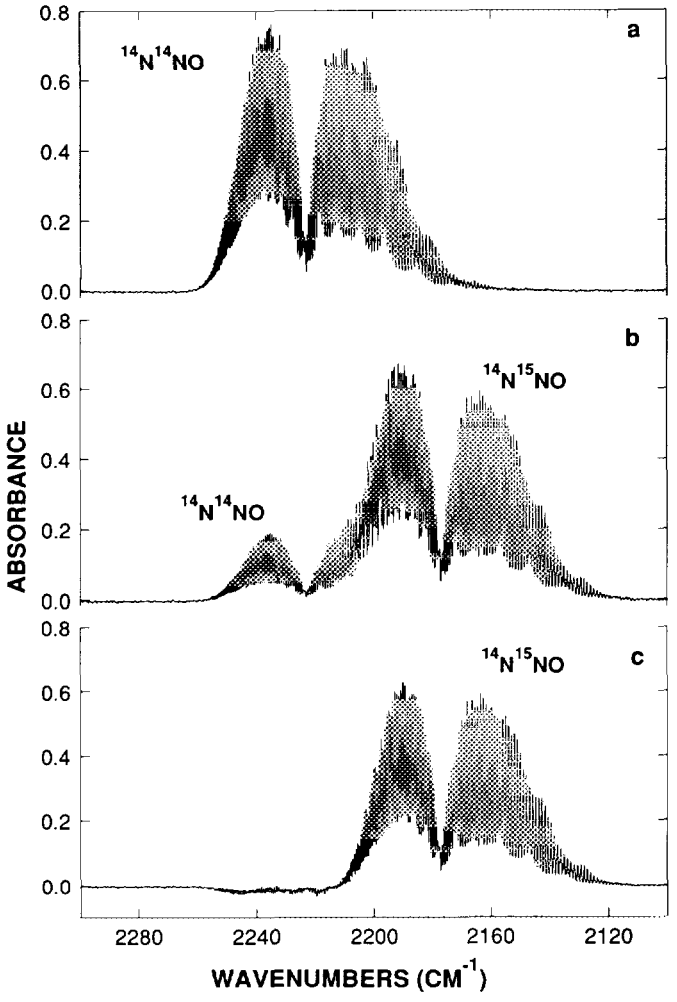

FIG. 3. Gas phase FTIR spectra of nitrous oxide in the 2100–2300 cm^{-1} region for the reaction of nitric oxide and ammonia over amorphous chromia at 195°C in the presence of 1.8% O_2. (a) Product of reaction of ^{14}NO and $^{14}NH_3$; (b) product of reaction of ^{15}NO and $^{14}NH_3$; (c) difference spectrum: spectrum (b) minus ≈15% of spectrum (a).

exception appears to be the $^{15}N_2$ species. As previously noted, accurate determination of $^{15}N_2$ is difficult for experiments with excess oxygen due to the coincidence of its mass spectral signal with that of ^{14}NO. The results for amorphous chromia and crystalline α-Cr_2O_3 scatter around zero, suggesting that no significant amounts of $^{15}N_2$ are produced in the presence of oxygen.

The final column in Tables 1 and 2 gives the amount of $^{14}N^{15}NO$ as a percentage of the mixed species, i.e., ($^{14}N^{15}N$ + $^{14}N^{15}NO$). Figure 4 shows clearly how this value increases with temperature for both forms of chromia, $^{14}N^{15}NO$ representing >75% of the mixed species at 280°C. Figure 4 also illustrates one special additional feature. At temperatures above 210°C, significant amounts of ^{14}NO were detected in the product gas by FTIR measurements. This must arise from ammonia oxidation, rather than exchange between ^{15}NO and $^{14}NH_3$, since no concurrent formation of $^{15}NH_3$ was detected.

Hence, for both chromia catalysts in the presence of oxygen, nitrous oxide is largely derived from a combination reaction between the two reactants. The increasing amount of ammonia oxidation which occurs at higher temperatures preferentially forms nitrogen, not nitrous oxide.

Absence of Oxygen

A similar series of isotopic labeling experiments were carried out for the reaction of ^{15}NO and $^{14}NH_3$ in the absence of oxygen. The primary data obtained are given in Table 3. There is one special feature for reaction at the highest temperature used (i.e., 350°C). As reported previously for both chromia and V_2O_5/TiO_2 catalysts (18), the formation of $^{15}NH_3$ can be inferred from mass balance calculations and directly measured by FTIR spectroscopy. Formation of $^{15}NH_3$ is not due to exchange since no ^{14}NO is formed. Its source is likely to be a reaction between product water and a species formed by dissociation of ^{15}NO (15).

Figure 5 summarizes the isotopic distributions calculated for nitrous oxide from the data of Table 3. The results are quite unlike those in Fig. 1 for reaction in the presence of oxygen. Doubly labeled nitrous oxide, $^{15}N_2O$, which must arise from ^{15}NO alone, is now the dominant form over crystalline α-Cr_2O_3 under all conditions. It is also formed in the greatest amount when using amorphous chromia at temperatures below 300°C, above which it falls slightly below $^{14}N^{15}NO$. Formation of $^{14}N_2O$ is negligible with both catalysts. The distribution of nitrous oxides was

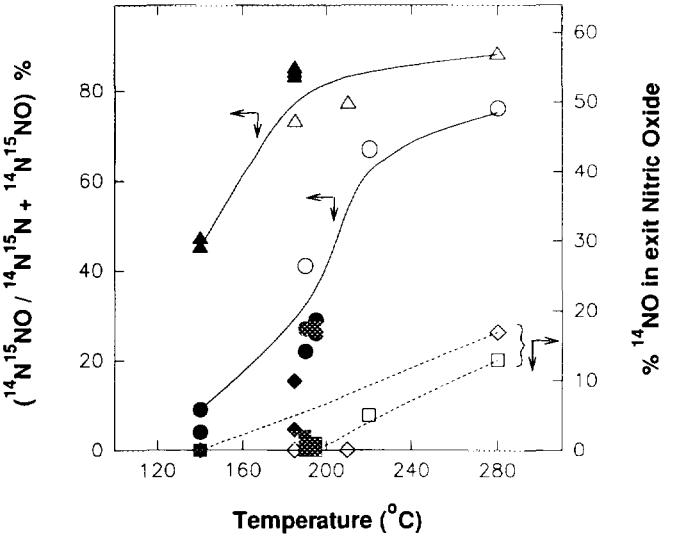

FIG. 4. Selectivity to $^{14}N^{15}NO$ as a percentage of the mixed species ($^{14}N^{15}N$ + $^{14}N^{15}NO$) and percentage of ^{14}NO in the exit nitric oxide as a function of temperature. Filled symbols are for 1.8% O_2; open symbols are for ≈1000 ppm O_2. Crystalline α-Cr_2O_3: selectivities (▲, △) and ^{14}NO percentages (◆, ◇). Amorphous chromia: selectivities (●, ○) and ^{14}NO percentages (■, □).

TABLE 3

Isotopic Product Distributions for the Reaction of ^{15}NO and $^{14}NH_3$ in the Absence of Oxygen over Amorphous Chromia and α-Cr_2O_3

Catalyst	Temp. (°C)	Mass of catalyst (mg)	Flow rate (ml/min)	Conversion (%) ^{15}NO	Conversion (%) $^{14}NH_3$	Selectivity to N_2O^a (%)	Product distribution (ppm) $^{14}N_2$	$^{14}N^{15}N$	$^{15}N_2$	$^{14}N_2O$	$^{14}N^{15}NO$	$^{15}N_2O$	$^{15}NH_3{}^b$ (mass balance)	$^{15}NH_3$ (FTIR)	$^{14}N^{15}NO/(^{14}N^{15}N + {}^{14}N^{15}NO)$ (%)
Amorphous chromia	195	100	40	32	12	66	30	49	−4	0	67	88	—	<5	58
		300	33	71	17	72	56	81	−13	4	141	202	—	<5	64
	220	50	40	38	13	60	51	70	−10	0	90	91	—	<5	56
		200	40	75	25	70	66	89	−20	3	147	220	—	<5	62
	280	50	120	42	23	55	7	98	21	0	74	79	—	<5	43
		100	60	72	34	53	24	160	31	3	103	139	—	<5	39
	350	50	80	62	38[c]	14	44	235	83	1	32	22	78	49	12
α-Cr_2O_3	220	80	60	28	14	50	0	68	3	0	32	69	—	<5	32
		200	40	46	15	61	−2	106	−5	4	47	116	—	<5	31
		450	33	69	24	64	−12	153	−13	4	77	190	—	<5	33
	280	50	200	38	25	48	3	142	0	2	21	115	—	<5	13
		100	120	75	40	45	10	237	8	2	39	161	—	<5	14
		100	33	83	44	34	60	267	21	0	40	135	—	<5	13
	350	50	120	84	48[c]	12	61	355	79	0	16	50	112	30	4

[a] Selectivity is defined as $(N_2O/(N_2 + N_2O + {}^{14}NO))$. Negatives are not included in the calculation.
[b] "—" means that $^{15}NH_3$ was not calculated from the mass balance because $^{15}NH_3$ was less than the FTIR detection limit of 5 ppm.
[c] $^{14}NH_3$ conversion determined by FTIR spectroscopy.

also confirmed by FTIR spectroscopy, as shown in Fig. 6. Figure 6b shows the absorbance spectrum of the product gas from the reaction of ^{15}NO and $^{14}NH_3$ over amorphous chromia in the absence of oxygen at 220°C. The two overlapping features centered at 2177.7 and 2154.7 cm^{-1} can be assigned to $^{14}N^{15}NO$ and $^{15}N_2O$, respectively (16). Note that Tables 1 and 2 show that no $^{15}N_2O$ is produced for chromia catalysts in the presence of oxygen. Thus, oxygen concentrations of ≈1000 ppm are obviously sufficient to prevent the NO decomposition reaction producing $^{15}N_2O$, which occurs in the absence of oxygen over both morphologies of chromia.

The isotopic distributions for nitrogen obtained from Table 3 are shown in Fig. 7. Unlike the situation for reaction in the presence of oxygen, the combination reaction to $^{14}N^{15}N$ is the dominant route to nitrogen under all conditions with both catalysts. Also, unlike reaction in the presence of oxygen, some nitric oxide decomposition to $^{15}N_2$ is evident at the higher temperatures. Ammonia oxidation is generally small, with the apparent exception of reaction at the two lower temperatures with the amorphous catalyst when $^{14}N_2$ reaches 40%. However, those results may not be entirely reliable, since as noted before, mass spectral determinations of low $^{14}N_2$ concentrations (as here) are difficult due to the necessity for a substantial background correction.

In contrast to the results in excess oxygen, the amount of $^{14}N^{15}NO$ as a percentage of the total mixed products

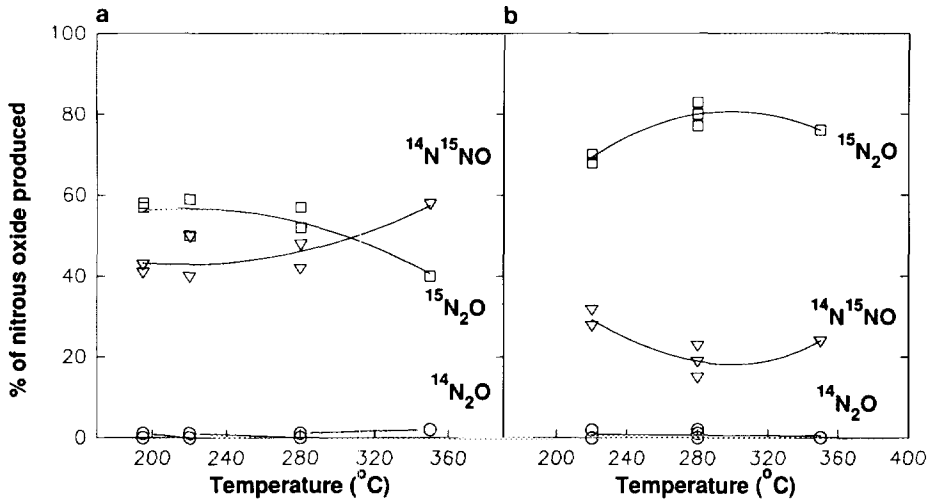

FIG. 5. Internal distribution of the nitrous oxides in the absence of oxygen as a function of temperature ((○) $^{14}N_2O$; (▽) $^{14}N^{15}NO$; (□) $^{15}N_2O$) over (a) amorphous chromia and (b) α-Cr_2O_3.

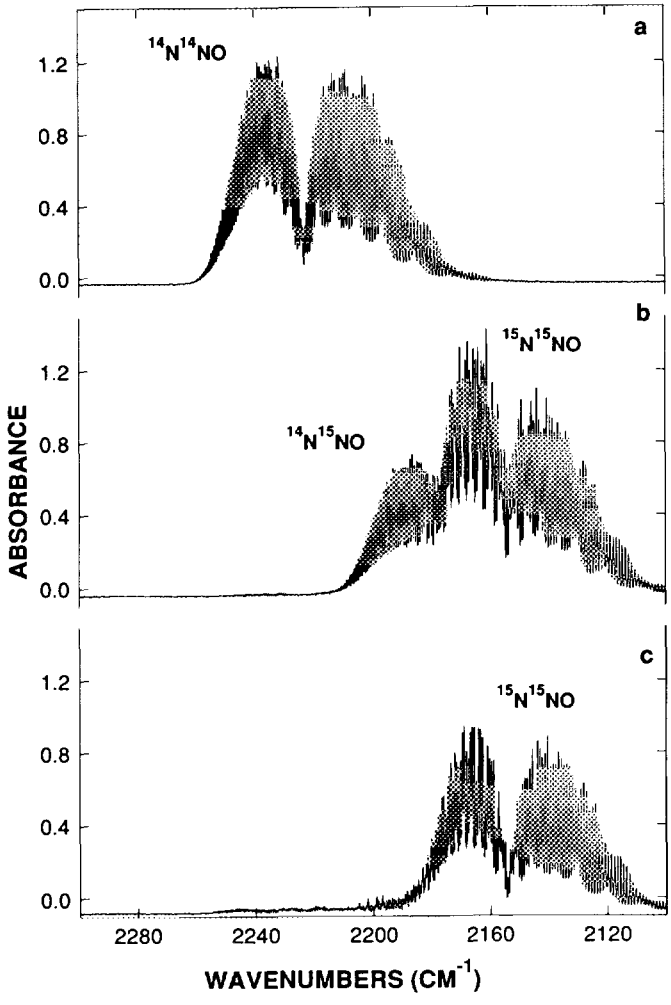

FIG. 6. Gas phase FTIR spectra of nitrous oxide in the 2100–2300 cm^{-1} region for the reaction of nitric oxide and ammonia over amorphous chromia at 220°C in the absence of gas phase O_2. (a) Product of reaction of ^{14}NO and $^{14}NH_3$; (b) product of reaction of ^{15}NO and $^{14}NH_3$; (c) difference spectrum: spectrum (b) minus the features due to $^{14}N^{15}NO$.

($^{14}N^{15}N$ + $^{14}N^{15}NO$) decreases with increasing temperature. The amount of $^{15}N_2O$ produced also decreases with reaction temperature, and a corresponding increase in the amount of $^{15}N_2$ formed is observed. Figure 8 shows the distribution of all species as a percentage (mol%) of the total products and clearly shows how the nitrogen production increases and the nitrous oxide formation decreases with increasing temperature. This observation will be discussed in more detail later in the paper.

Comparison with Earlier Studies

It is of interest to compare the isotopic distributions found here with previous results for chromia systems (carried out under very different conditions) and with the only previous studies (on vanadia systems) under similar conditions. Table 4 summarizes the earlier findings. Since some studies used $^{14}NO/^{15}NH_3$ mixtures rather than $^{15}NO/^{14}NH_3$, the results are expressed in terms of source rather than isotopic distribution. The results for vanadia systems are clear-cut. Nitrogen, the dominant product over all the supported catalysts, is derived very largely by the combination reaction [1]. Nitrous oxide, which is more evident with pure vanadia and with supported catalysts having high vanadia contents, is produced by the corresponding reaction [2]. The results of Janssen *et al.* (8), for O_2 concentrations of about 500 ppm, show some direct conversion of nitric oxide to nitrogen. Those authors specifically rule out any ammonia oxidation under their conditions. By contrast, the experiments of Vogt *et al.* (9, 10) show no nitric oxide decomposition, but significant ammonia oxidation, especially over a 9.5% V_2O_5/85.5% SiO_2/5% TiO_2 catalyst. These differences may arise because of the much higher oxygen concentrations (2%) used in the latter studies.

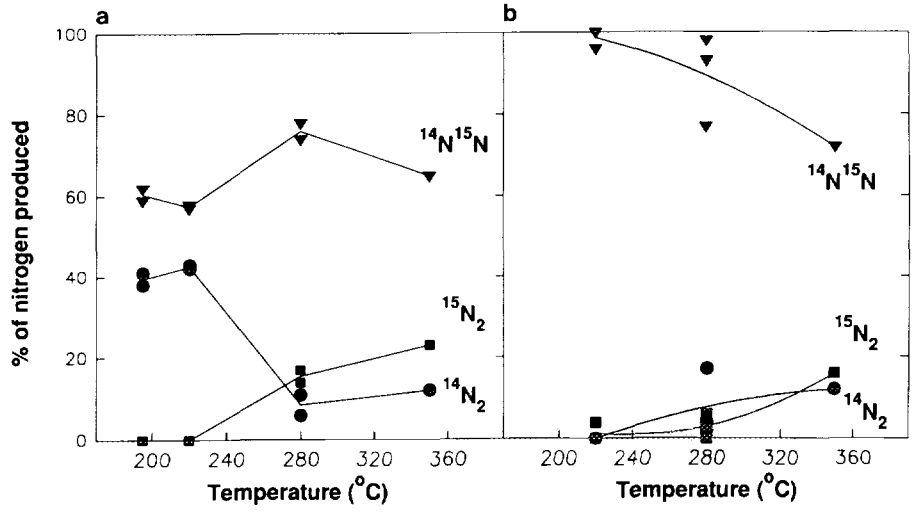

FIG. 7. Internal distribution of the nitrogens in the absence of oxygen as a function of temperature ((●) $^{14}N_2$; (▼) $^{14}N^{15}N$; (■) $^{15}N_2$) over (a) amorphous chromia and (b) α-Cr_2O_3.

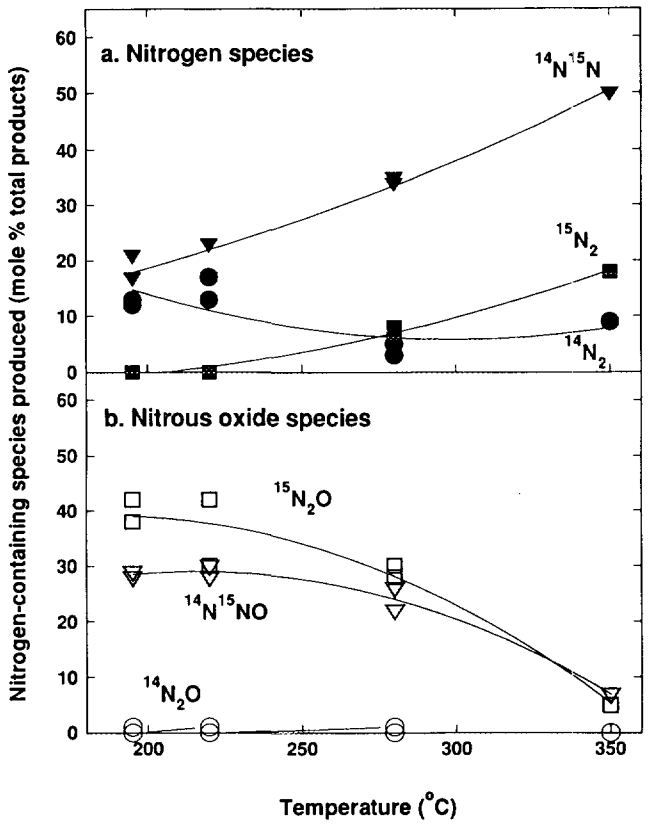

FIG. 8. (a) Nitrogen and (b) nitrous oxide species as a percentage of the total nitrogen-containing products ((●) $^{14}N_2$; (▼) $^{14}N^{15}N$: (■) $^{15}N_2$; (○) $^{14}N_2O$; (▽) $^{14}N^{15}NO$; (□) $^{15}N_2O$) as a function of temperature for reaction in the absence of oxygen over amorphous chromia.

The present results for the NO + NH_3 reaction over chromia in the presence of oxygen resemble the above pattern, especially for bulk and bulk-like vanadia, but with a greater tendency to oxidize ammonia to nitrogen alone. The similarity is greatest between the behavior of amorphous chromia below 200°C and the results of Vogt *et al.* (9) for a V_2O_5/SiO_2 catalyst having high vanadia content (44% V_2O_5). Both exhibit moderate selectivity to nitrous oxide (compare Tables 1 and 2 to Table 4) and some ammonia oxidation to nitrogen (Fig. 2a), but not to nitrous oxide (Fig. 1a). The higher oxidation power of amorphous chromia is very evident by 280°C when the fraction of nitrogen derived from ammonia oxidation is already twice that for V_2O_5/SiO_2 at 400°C, even though the oxygen pressure used in the latter case was much higher (18,000 ppm versus ~1000 ppm). When low oxygen pressures are used with bulk vanadia, as in the experiments of Janssen *et al.* (8), there is no ammonia oxidation at all for temperatures below 400°C. Crystalline chromia is still more prone to oxidize ammonia, with 75% of the nitrogen derived in that way at 200°C (Fig. 2b).

The results of Niiyama *et al.* (12) for reaction over crystalline chromia and chromia/alumina at high pressure in the absence of oxygen show a very different picture. Large amounts of nitrous oxide derive both nitrogen atoms from nitric oxide. Our results for reaction in the absence of oxygen (Fig. 5) confirm this behavior for both amorphous and crystalline chromia. Indeed, $^{15}N_2O$ is the largest single nitrogen-containing product under some conditions (Table 3).

Mechanistic Implications

The present isotope experiments were designed to reveal the origin of the nitrogen atoms incorporated in the nitrogen-containing products, and do not in themselves provide definitive pointers to the steps by which they are made on chromia surfaces. Nonetheless, some comments are warranted. There are four major products: $^{14}N^{15}N$, $^{14}N^{15}NO$, $^{14}N_2O$, and $^{14}N_2$. Under some conditions, $^{14}N_2O$ and $^{15}N_2$ are also significant products.

The reaction of NO and NH_3, particularly over vanadia-based catalysts, has been extensively studied, but a generally accepted mechanism has failed to emerge. There are abundant, though conflicting, spectroscopic investigations (18–23) of the adsorbed state of ammonia on vanadia-based catalysts. Some workers have found that NH_3 absorbs on Brønsted acid sites as NH_4^+ groups, while others have shown that ammonia adsorbs on Lewis acid sites as NH_i type species (i = 0–3). Similarly, convincing spectroscopic evidence for adsorbed NO on SCR catalysts under reaction conditions when NH_3 is present has not been reported. However, the observation (8, 24) that NO is converted to $N^{18}O$ by exchange with $^{18}O_2$ does provide evidence for adsorbed NO.

It seems unlikely that NO can react directly with NH_4^+ to produce N_2, since the rearrangement necessary seems improbable. The most common view is that N_2 formation arises from the reaction of an NH_i (i = 1, 2) species and either adsorbed or gas phase NO, and the following reaction has recently been suggested (25):

$$^{14}NH_2(a) + {}^{15}NO(a) \rightarrow {}^{14}N^{15}N + H_2O. \quad [3]$$

This reaction is analogous to the elementary, purely gas phase reaction thought responsible for N_2 formation in the thermal $DeNO_x$ process (26).

Thus, one possible model for nitrogen formation over chromia catalysts, consistent with the overall stoichiometry of reaction [1], is

$$Cr{=}O + {}^{14}NH_3(a) \rightarrow Cr{-}OH + {}^{14}NH_2(a) \quad [4]$$

$$^{14}NH_2(a) + {}^{15}NO(a) \rightarrow {}^{14}N^{15}N + H_2O. \quad [5]$$

The elimination of water follows,

$$2Cr{-}OH \rightarrow Cr{=}O + Cr\square + H_2O \quad [6]$$

TABLE 4

Summary of Previous Isotopic Results for the Source of Nitrogen and Nitrous Oxide from the NO + NH_3 Reaction

Reference	Catalyst	Temp. (°C)	Partial pressures (atm × 10^{-6})			Selectivity	Source of N_2 (%)			Source of N_2O (%)		
			O_2	NO	NH_3	N_2O (%)	NH_3 alone	NO + NH_3	NO alone	NH_3 alone	NO + NH_3	NO alone
Janssen *et al.* (8)	V_2O_5	400	495	500	473	66	—	82	18	—	93	7
	$V_2O_5/SiO_2/Al_2O_3$	400	495	500	473	8	—	94	6	—	100	—
	V_2O_5/Al_2O_3	400	495	500	473	4	—	96	4	—	100	—
	V_2O_5/TiO_2	400	495	500	473	25	—	97	3	—	89	11
Vogt *et al.* (9, 10)	V_2O_5/TiO_2	400	20,000	500	500	9	6	94	—	—	100	—
	$V_2O_5/SiO_2/TiO_2$[a]	400	20,000	500	500	6	37	63	—	50	50	—
	$V_2O_5/SiO_2/TiO_2$[b]	400	20,000	500	500	2	15	85	—	33	67	—
	V_2O_5/SiO_2[c]	400	20,000	500	500	40	18	82	—	8	92	—
Niiyama *et al.* (12, 13)	Cr_2O_3/Al_2O_3 (reduced)	200	nil	132,000	66,000	21	—	50	50	—	—	100
	(NO + NH_3)	200	nil	132,000	66,000	22	—	88	12	—	—	100
	α-Cr_2O_3 (reduced)	200	nil	132,000	66,000	40	—	100	—	—	14	86
	(NO + NH_3)	200	nil	132,000	66,000	40	—	100	—	—	14	86
	α-Cr_2O_3 (preoxidized)	200	nil	132,000	66,000	9	—	100	—	—	87	13
	(NO + NH_3)	200	nil	132,000	66,000	33	—	100	—		39	61
	α-Cr_2O_3 (preoxidized)	150	nil	197,000	197,000	18	—	86	14	—	73	27

[a] 9.5% V_2O_5/85% SiO_2/5% TiO_2.
[b] 6% V_2O_5/33% SiO_2/61% TiO_2.
[c] 44% V_2O_5/55% SiO_2.

(where Cr□ is a reduced surface site), and if oxygen is present, the rapid reoxidation of the surface occurs,

$$2Cr\square + O_2 \rightarrow 2Cr{=}O. \quad [7]$$

If the dehydration step of Eq. [6] is slow compared to the reoxidation process described in Eq. [7], then in the presence of oxygen, the vacancy concentration would be low and the catalyst would be in a highly oxidized state. However, in the absence of gas phase oxygen, reaction [7] does not occur and the concentration of chromyl groups, which are necessary for the hydrogen abstraction process described in Eq. [4], will be low. Thus, this model is consistent with the observation that small quantities of O_2 have a large effect on the rate of the SCR reaction.

The formation of $^{14}N^{15}NO$ has received less attention since temperatures above 350°C are required for its formation over vanadia-based catalysts. A number of mechanisms have been proposed for V_2O_5 based catalysts (20, 25, 28). Went *et al.* (25) suggested that the reaction proceeds through an NH_2(a) species in a similar way to that proposed for nitrogen formation (compare [3]):

$$NH_2(a) + NO(a) + V_mO_{2.5m} \rightarrow N_2O(g) + H_2O(g) + V_mO_{(2.5m-1)}. \quad [8]$$

It is possible that the formation of $^{14}N^{15}NO$ over chromia catalysts occurs via a similar process to that of Eq. [8].

Another possibility is that higher temperatures and catalysts with greater oxidizing (hydrogen abtracting) power favor the further dissociation of NH_2 groups to NH species. Nitrous oxide may then be produced by reaction between an NH species and NO:

$$^{14}NH(a) + {}^{15}NO(a) + Cr{=}O \rightarrow {}^{14}N^{15}NO + Cr\text{–}OH. \quad [9]$$

Went *et al.* (27) have presented evidence for adsorbed NH_2 and NH species formed by dissociative adsorption on vanadium oxide catalysts using Laser Raman spectroscopy. It is possible that these species also exist on chromium oxide catalysts. An earlier study (7) of chromia catalysts showed that the surface oxygen on α-Cr_2O_3 has greater oxidizing (hydrogen abstracting) potential than that of amorphous chromia. Thus, as observed (see Fig. 4), higher temperatures and greater hydrogen abstracting power (as in the case of α-Cr_2O_3 (7)) result in higher selectivities to $^{14}N^{15}NO$.

Formation of NH groups may also account for the observation of the ammonia oxidation products, $^{14}N_2$ and ^{14}NO:

$$^{14}NH(a) + {}^{14}NH(a) + 2Cr{=}O \rightarrow {}^{14}N_2 + 2Cr\text{–}OH \quad [10]$$

$$^{14}NH + 2Cr{=}O \rightarrow {}^{14}NO + Cr\text{–}OH + Cr\square \quad [11]$$

These reactions are analogous to the gas phase processes for the formation of these products (26). Complete stripping of the ammonia to form an adsorbed N species may also play a role in the formation of the ammonia oxidation product ^{14}NO:

$$^{14}N(a) + Cr{=}O \rightarrow {}^{14}NO + Cr\square \qquad [12]$$

A step similar to Eq. [12] has previously been suggested to account for ammonia oxidation to NO over vanadia-containing catalysts (29). The fact that ammonia oxidation is more significant with crystalline chromia is consistent with this model since it is this morphology which has surface oxygen species with greater oxidizing (hydrogen abstracting) power (7). This model would also account for the apparent relationship between high selectivities to N_2O and high activities for ammonia oxidation.

It should be noted that significant concentrations of $^{14}N_2O$ are only observed when ^{14}NO is also present in the exit gases. It is possible that the $^{14}N_2O$ arises from reaction of ^{14}NO, formed from a process similar to [11] or [12], with NH_2 or NH according to [8] or [9]. Nitrogen produced from ammonia oxidation, $^{14}N_2$, by contrast, can be present in significant concentrations in the absence of $^{14}N_2O$, suggesting a direct route to its formation involving a combination of species which are more hydrogen deficient than NH_2. Reaction [10] is a possibility for such a process.

In the absence of oxygen, the surface of the catalyst will be more reduced, having a higher population of vacancies ($Cr\square$) and a lower number of Cr=O groups. Reoxidation of the catalyst surface must be achieved by NO rather than gas phase molecular oxygen. It has been previously suggested (12, 25) that the NO decomposition reactions are a means of reoxidizing the catalyst surface. Observations of dimeric NO species adsorbed on α-Cr_2O_3 (20) and supported chromia (31, 32) surfaces, as well as other reports of *dinitrosyl* species (33, 34), provide a possible mechanism for the formation of $^{15}N_2O$:

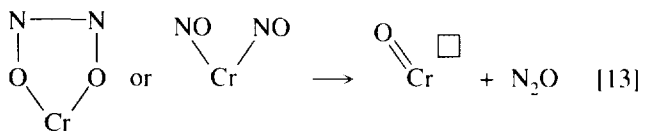

[13]

Alternatively, dissociation of NO on reduced surface sites may provide another possible route to the formation of $^{15}N_2O$:

$$^{15}NO + Cr\square \rightarrow Cr{=}O + {}^{15}N(a) \qquad [14]$$

$$^{15}N(a) + {}^{15}NO \rightarrow {}^{15}N_2O \qquad [15]$$

There are two additional features of the reactions in the absence of oxygen which are worthy of comment. The increased production of $^{14}N^{15}N$ with temperature over both chromia morphologies is accompanied by a decrease in the amount of $^{14}N^{15}NO$ formed. The amount of $^{15}N_2$ produced also increases with reaction temperature, and a corresponding decrease in the amount of $^{15}N_2O$ formed is observed. There are at least two plausible explanations. The products $^{14}N^{15}N$ and $^{14}N^{15}NO$ and $^{15}N_2$ and $^{15}N_2O$ may arise from common intermediate complexes, the relative split to the different species changing with reaction temperature. Another possible explanation is the further interaction of the $^{14}N^{15}NO$ and $^{15}N_2O$ molecules with the catalyst surface leading to a loss of oxygen from the nitrous oxides species and the concomitant formation of the respective nitrogens, i.e., $^{14}N^{15}N$ and $^{15}N_2$. The latter possibility was checked by performing an experiment in which N_2O and NH_3 were fed to crystalline chromia. Results for N_2 and N_2O concentrations as a function of temperature are given in Fig. 9. It is clear that significant conversion of N_2O to N_2 occurs; however, some NH_3 conversion to N_2 also takes place, and the overall reaction may be represented by a two step process,

$$3N_2O + 3Cr\square \rightarrow 3N_2 + 3Cr{=}O \qquad [16]$$

$$2NH_3 + 3Cr{=}O \rightarrow N_2 + 3H_2O + 3Cr\square, \qquad [17]$$

with the overall reaction conforming to

$$3N_2O + 2NH_3 \rightarrow 4N_2 + 3H_2O. \qquad [18]$$

Concentrations of N_2 calculated using the stoichiometry of Eq. [18] for the given amounts of N_2O converted

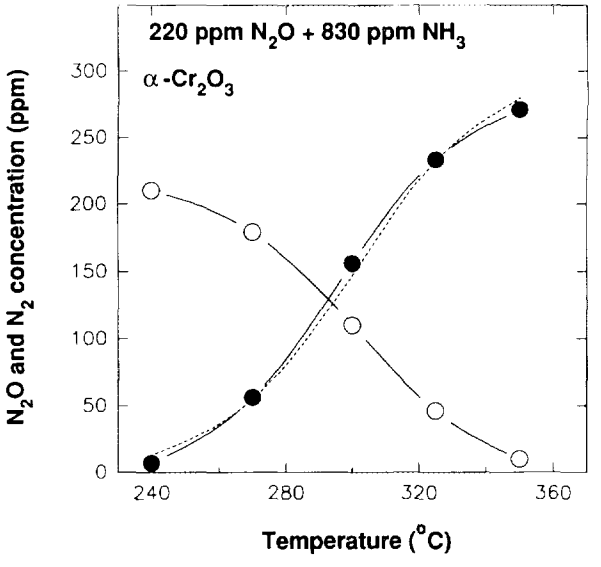

FIG. 9. N_2O (○) and N_2 (●) concentrations for the reaction of N_2O (220 ppm) and NH_3 (830 ppm) over α-Cr_2O_3 as a function of temperature. Dashed line calculated on the basis of reaction [18].

(dashed line in Fig. 9) are in excellent agreement with those observed experimentally. Note that N_2O alone does not interact with the catalyst to form N_2, even at 350°C, implying that a reduced surface, produced by NH_3, is required for the reaction [16] to occur.

The second feature of the reaction in the absence of O_2 is the formation of $^{15}NH_3$. At 350°C, small amounts of this product are observed over both amorphous and crystalline chromia (11 and 5 mol% of nitrogen-containing products, respectively). This represents a direct conversion of ^{15}NO to $^{15}NH_3$ and not an exchange process, since under these conditions no ^{14}NO is observed by FTIR spectroscopy. For V_2O_5/TiO_2 catalysts at 350°C, $^{15}NH_3$ has been found to comprise ≈20% of the total nitrogen-containing species (15). Previous labeling studies have also demonstrated that NO decomposition to $^{15}N_2$ and $^{15}N_2O$ is negligible over titania-supported vanadia catalysts (8, 15) in the absence of oxygen, even at 450°C. Thus, for chromia catalysts in the absence of gas phase oxygen, reoxidation of the catalyst surface occurs mainly via NO decomposition reactions to $^{15}N_2$ and $^{15}N_2O$, whereas, for supported vanadia catalysts the direct conversion (15) of ^{15}NO to $^{15}NH_3$ is the predominant route.

Better elucidation of the mechanisms which occur on chromia catalysts in the presence and absence of oxygen will require direct observation of the surface species under reaction conditions.

CONCLUSIONS

Isotopic labeling studies of the SCR reaction between ^{15}NO and $^{14}NH_3$ have been performed for two forms of chromia catalysts. The results show that:

1. In the presence of excess (1.8%) O_2, and at sufficiently low temperature, the combination reaction producing nitrogen predominates. Thus, $^{14}N^{15}N$ is the major product below 200°C with amorphous chromia, and below 150°C with α-Cr_2O_3.

2. Some ammonia oxidation to produce $^{14}N_2$ rather than $^{14}N_2O$ proceeds in parallel with the combination reaction when oxygen is present. Ammonia oxidation increases with increasing temperature and is considerably more pronounced with crystalline chromia than with amorphous chromia. Thus, at ≈200°C $^{14}N^{15}N$ is the major form of nitrogen observed over amorphous chromia, whereas, crystalline α-Cr_2O_3 produces nitrogen largely by ammonia oxidation.

3. At higher temperatures in the presence of oxygen, production of $^{14}N^{15}NO$ becomes significant. This product is always the most abundant nitrous oxide, and hence the undesirable formation of nitrous oxide arises from the reaction of NO and NH_3 and not from ammonia oxidation. No evidence of $^{14}N^{15}NO$ was observed by FTIR spectroscopy, indicating preservation of the N–O bond of the nitric oxide molecule.

4. In the absence of oxygen the reaction between ^{15}NO and $^{14}NH_3$ is much slower. Under these conditions the isotopic product distributions over the two forms of chromia are very similar. Below 250°C $^{15}N_2O$, reflecting NO decomposition, is the largest nitrogen-containing product. At higher temperatures, the amounts of the nitrous oxides ($^{15}N_2O$ and $^{14}N^{15}NO$) decrease, and the amounts of their corresponding nitrogens ($^{15}N_2$ and $^{14}N^{15}N$) increase. One possible contributor is the decomposition of N_2O due to a reaction conforming to the following overall stoichiometry:

$$3N_2O + 2NH_3 \rightarrow 4N_2 + 3H_2O.$$

5. Small concentrations of oxygen (≈1000 ppm) are sufficient to prevent the formation of $^{15}N_2O$ which occurs in the absence of O_2. There is a threshold O_2 concentration above which further increases in the O_2 concentration have little influence on the product distribution.

6. Tentative mechanisms have been proposed for the formation of the major products, but the detailed steps in these processes have yet to be positively identified.

ACKNOWLEDGMENTS

This project is supported by NERDDC/ACARP (Project 1584) and the CSIRO/UNSW Collaborative Research Fund. One of us (B.L.D.) acknowledges support from the Commonwealth Government APRA scholarships. We thank Martin Kelly and Alan McCutcheon for their help with the construction of the apparatus.

REFERENCES

1. Bosch, H., and Janssen, F. J. J. G., *Catal. Today* **2,** 369 (1988).
2. Curry-Hyde, H. E., and Baiker, A., *Ind. Eng. Chem. Res.* **29,** 1985 (1990).
3. Curry-Hyde, H. E., Musch, H., and Baiker, A., *Appl. Catal.* **65,** 211 (1990).
4. Kobylinski, T. P., and Taylor, B. W., *J. Catal.* **31,** 450 (1973).
5. Niiyama, H., Murata, K., Ebitani, A., and Echigoya, E., *J. Catal.* **48,** 194 (1977).
6. Wong, W. C., and Nobe, K., *Ind. Eng. Chem. Prod. Res. Dev.* **25,** 179 (1986).
7. Curry-Hyde, H. E., Musch, H., Baiker, A., Schraml-Marth, M., and Wokaun, A., *J. Catal.* **133,** 397 (1992).
8. Janssen, F. J. J. G., van den Kerkhof, F. M. G., Bosch, H., and Ross, J. R. H., *J. Phys. Chem.* **91,** 6633 (1987).
9. Vogt, E. T. C., Bott, A., van Dillen, A. J., Geus, J. W., Janssen, F. J. J. G., and van den Kerkhof, F. M. G., *J. Catal.* **114,** 313 (1988).
10. Vogt, E. T. C., Boot, A., van Dillen, A. J., Geus, J. W., and Janssen, F. J. J. G., *Catal. Today* **2,** 569 (1988).
11. Niiyama, H., Ookawa, T., and Echigoya, E., *Nippon Kagaku Kaishi* **11,** 1871 (1975).
12. Niiyama, H., Murata, K., and Echigoya, E., *J. Catal.* **48,** 201 (1977).
13. Niiyama, H., Murata, K., Can, H. V., and Echigoya, E., *J. Catal.* **62,** 1 (1980).

14. Miyamoto, A., Kobayashi, K., Inomata, M., and Murakami, Y., *J. Phys. Chem.* **86,** 2945 (1982).
15. Duffy, B. L., Curry-Hyde, H. E., Cant, N. W., and Nelson, P. F., *J. Phys. Chem.* **97,** 1729 (1993).
16. Pinchas, S., and Laulicht, I., "*Infrared Spectra of Labelled Compounds*." Academic Press, New York, 1971.
17. Amiot, C., *J. Mol. Spectrosc.* **59,** 191 (1976).
18. Takagi, M., Kawai, T., Soma, M., Onishi, T., and Tamaru, K., *J. Catal.* **50,** 441 (1977).
19. Topsøe, N.-Y., and Topsøe, H., *Catal. Today* **9,** 77 (1991).
20. Topsøe, N.-Y., Slabiak, T., Clausen, B. S., Srnak, T. Z., and Dumesic, J. A., *J. Catal.* **134,** 742 (1992).
21. Rajadhyaksha, R. A., Hausinger, G., Zeilinger, H., Ramstetter, A., Schmelz, H., and Knözinger, H., *Appl. Catal.* **51,** 67 (1989).
22. Rajadhyaksha, R. A., and Knözinger, H., *Appl. Catal.* **51,** 81 (1989).
23. Kantcheva, M. M., Hadjiivanov, K. I., and Klissurski, D. G., *J. Catal.* **134,** 299 (1992).
24. Janssen, F. J. J. G., van den Kerkhof, F. M. G., Bosch, H., and Ross, J. R. H., *J. Phys. Chem.* **91,** 5921 (1987).
25. Went, G. T., Leu, L.-J., Rosin, R. R., and Bell, A. T., *J. Catal.* **134,** 492 (1992).
26. Miller, J. A., and Bowman, C. T., *Prog. Energy Combust. Sci.* **15,** 287 (1989).
27. Went, G. T., and Bell, A. T., *Catal. Lett.* **11,** 111 (1991).
28. Odenbrand, C. U. I., Gabrielsson, P. L. T., Brandin, J. G. M., and Andersson, L. A. H., *Appl. Catal.* **78,** 109 (1991).
29. Went, G. T., Leu, L. J., Lombardo, S. J., and Bell, A. T., *J. Phys. Chem.* **96,** 2235 (1992).
30. Kugler, E. L., Kadet, A. B., and Gryder, J. W., *J. Catal.* **41,** 72 (1976).
31. Kugler, E. L., Kokes, R. J., and Gryder, J. W., *J. Catal.* **36,** 142 (1975).
32. Peri, J. B., *J. Phys. Chem.* **78,** 588 (1974).
33. Ghiotti, G., Garrone, E., Della Gatta, G., Fubini, B., and Giamello, E., *J. Catal.* **80,** 249 (1983).
34. Batis, H., Younes, M. K., and Ghorbel, A., *Bull. Soc. Chim. Belg.* **99,** 221 (1990).